Egyptian Geophysical Society
EGS Journal, Vol. 14, No. 1, 63-70 (2016)

POTENTIAL FIELD DATA INTERPRETATION OF STRUCTURAL SETTING OF WADI EL-RAYAN AND BAHARIYA OASIS AREA, NORTH WESTERN DESERT, EGYPT

Sh.M. Sharafeldin[(1)], A.R. Aboezz[(1)], K. Farhoud[(2)] and M. Elkammar[(1)]

(1) Geophysics Department, Cairo University, Egypt.
(2) Former Exploration Manager Gujarat Company.

تأويلات لبيانات الجهد الحقلى للوضع التركيبى لوادى الريان والواحات البحرية، شمال الصحراء الغربية، مصر

الخلاصة: يتضمن البحث دراسة بيانات طرق الجهد لمنطقة شمال الصحراء الغربية بمصر ودراسة خصائص الطبقات التحتية وتحديد المصايد التركيبية المختلفة حيث تم معالجة البيانات بفصل الشاذات الإقليمية عن المحلية باستخدام المرشحات مثل بتروورث ، جاوس ، المشتقات الرأسية الأولى والثانية والمشتقة الأفقية ثم تم تفسير البيانات بعد معالجتها كيفياً حيث تم إنشاء خريطة توضح الصدوع التى تؤثر فى المنطقة وخريطة أخرى توضح توزيع الخزانات فى منطقة الدراسة وكمياً حيث تم حساب العمق باستخدام طريقة أويلر كما تم عمل قطاع ثنائى الأبعاد لتحديد الفوالق فى القاعدة ورسم نموذج جيولوجى للبنية التحتية.

ABSTRACT: *The regional structural setting, sedimentary basins distribution and mapping the local structures of West Wadi El-Rayan area were delineated using potential field data. West Wadi El-Rayan lies as transit area between well known two major prolific sedimentary basins in the western desert (Egypt) which are represented by Gindi basin (Eocene basin) in the eastern side and Abu Gharadig basin (Early Cretaceous basin) in the western side.*
The Bouguer gravity and the total magnetic intensity (TMI) maps were digitized and gridded in 1000 m grid spacing before processing. The reduced to the pole (RTP) map was produced. The radially average power spectra for both the Bouguer and the RTP maps were calculated. Five different filters (Band pass, Gaussian, Butterworth filters, vertical and horizontal derivatives) were applied to produce the regional and residual maps. The processed maps revealed that NE-SW and NW-SE are the two main trends dominating the structures of the studied area. Several basins have been delineated in the area where the depth to basement ranges between 1000 and 5000 m. By integrating the results from different techniques, an interpreted basin distribution map was constructed where Abu-Gharadig, Gindi, Alam-Elbuieb, and Natrun basins were delineated. The depth to basement using different automatic techniques (Euler deconvolution and source parameter imaging; SPI) was calculated and adjusted by 2-D modeling along selected profiles. Interpretation of the potential field data help in delineating the main major structures in the north western desert which were formed by Jurassic-Early Cretaceous NE-SW normal faults and Late Cretaceous-Early Tertiary NW-SE compressional regime (wrench deformation with strike slip component). These are the two main trends dominating the structures of the studied area and define the expected sedimentary basins as Abu Gharadig, El Gindi, Alam Elbuieb , Natrun and Kattaniya high. The thickness of the sedimentary section was determined in each basin. Integrating the results from the processed magnetic and gravity maps, the depth-to-basement map and modeled profiles, an interpreted basin distribution map of the studied area was constructed showing different basin locations and their trends .

INTRODUCTION

The available magnetic data for this study include the total magnetic intensity map covering the northern Western Desert from latitude 28° 50' to 30° and longitude 28° 30' to 30° 45'and the Bouguer gravity map of the northern Western Desert from latitude 29° to 30° 30' and longitude 28° 20' to 30° 30'. The Bouguer gravity and total magnetic intensity maps from Meshref (1990) include the studied area. The West Wadi El-Rayan (WWER) area is located in the northern part of the Western Desert. It is bounded by latitudes 29º20' to 29º 50' N and longitudes 29º40' to30º 18'E (figure 1).

The structures within WWER area were controlled by reactivation of older faults in Jurassic-Early Cretaceous times (led to the development of NE-SW, NNE-SSW and ENE-WSW oriented normal faults and thickening of the Jurassic rocks against these faults) and Late Cretaceous/Early Tertiary events (led to the development of WNW-ESE and NW-SE oriented normal faults) that formed the Kattaniya inverted high that shaped the central part of WWER concession. Basin inversion led to serve erosion and downgrades the possibility of hydrocarbon charging for some parts in the West Wadi El-Rayan area from Jurassic/Cretaceous source rocks while positive effects of the inversion are expected in other parts within the concession as well (Moustafa, 2008).

The main target of the study, which is the determination of the basins distribution within the studied area. The Bouguer gravity and magnetic data were digitized and gridded before processing. Processing of both magnetic and gravity data was carried out using different frequency linear filtering techniques in order to achieve the main target. Moreover, a depth-to-basement map was produced from the reduced to pole (RTP) magnetic map which determines the thickness of the sediments within every basin in the studied area and,

hence, their relative possible potential prospectivity. 2-D magnetic modeling along selected profiles was carried out to confirm the basement depth and basin structural boundaries. Integrating the results from the processed magnetic and gravity maps, the depth-to-basement map, and the modeled profile; an interpreted basin distribution map of the studied area was constructed showing different basin locations and their trends in the studied area.

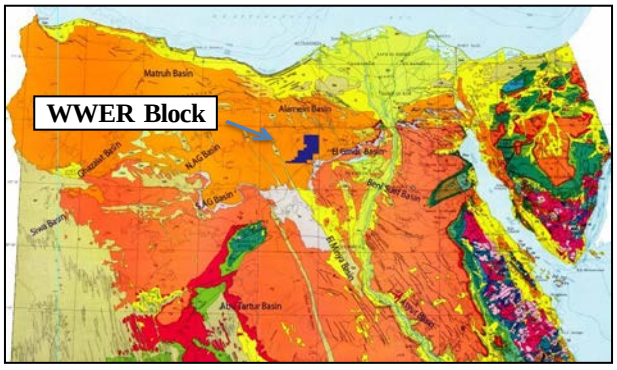

Figure (1): Location map of West Wadi El-Rayan area.

Processing of gravity and magnetic data:

The Bouguer gravity map (figure 2) and total magnetic intensity map were digitized and gridded with grid cell of 1000 meters. Reduction-to-pole (RTP) map (figure3) was produced to eliminated the doublet nature of magnetic anomalies**.** Potential field data is generally composed of regional and residual anomalies. A major step in the analysis of potential field data is the process of isolating the observed anomaly pattern into regional and residual components. This provides the interpreter with valuable information that helps in the delineation of the subsurface geological and structural setting in an area. The most common technique of separation of regional from residual component is through power spectral analysis of the potential field data. The products of these mathematically based anomaly removal processes visually enhance the data by making features easier to recognize; however, they all distort the results from being true magnetic or gravity measurements and this distortion must be appreciated before interpretation of such data is attempted (Blakely, 1995; Milligan and Gun, 1997).

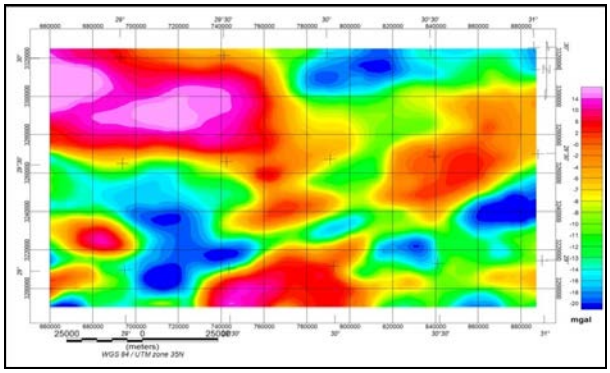

Figure 2: Bouguer gravity map of the studied area.

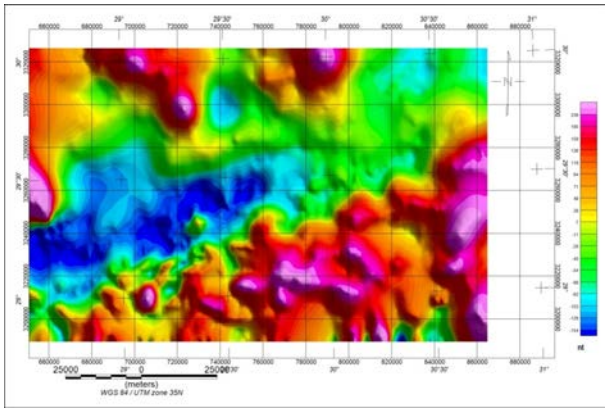

Figure (3): Reduced to the pole (RTP) magnetic map of the studied area.

Power spectrum of the RTP and Bouguer gravity data were calculated to determine the cut-off frequencies (figures 4 and 5, respectively).

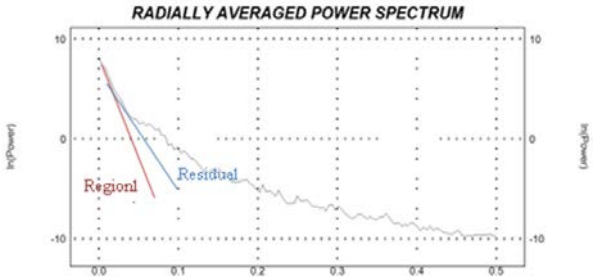

Figure (4): Radially averaged power spectrum for the RTP magnetic data showing the regional and residual components.

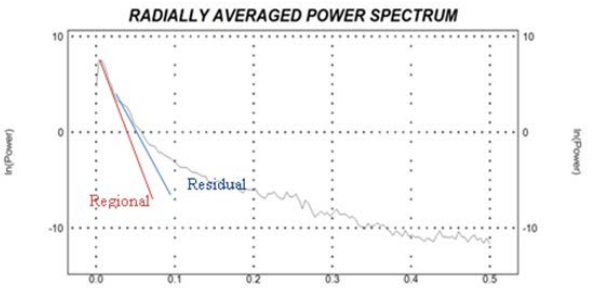

Figure (5): Radially averaged power spectrum for the Bouguer data showing the regional and residual components.

Gaussian, Butterworth, band pass and derivative filters were applied to the Bouguer gravity and the RTP magnetic maps to separate the different anomaly components. The best result was obtained with a Butterworth filter. The regional Butterworth maps of RTP magnetic and Bouguer gravity data are shown in Figures (6) and (7), respectively. The residual Butterworth maps of RTP magnetic and Bouguer gravity data are shown in Figures (8) and (9), respectively.

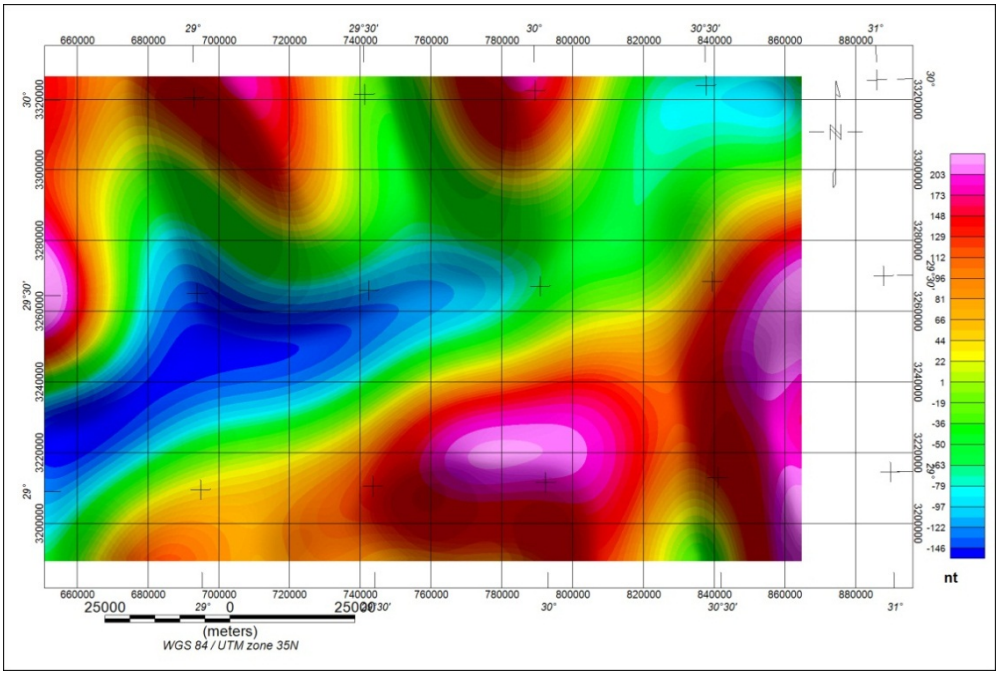

Figure 6: The regional RTP magnetic map after applying the Butterworth filter.

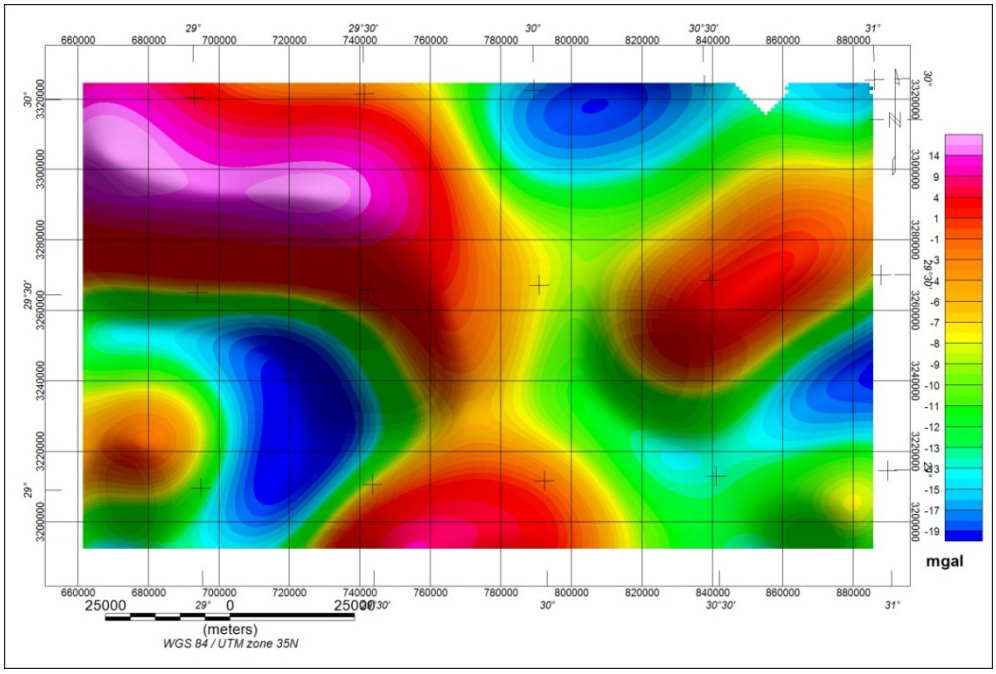

Figure 7: The regional Bouguer map after applying the Butterworth filter.

Euler deconvolution basement depth determination:

Thompson (1982), and Reid et al., 1990 showed that Euler in homogeneity relation could be written as:

$$(X - X_0)\frac{dT}{dx} + (y - y_0)\frac{dT}{dy} + (z - z_0)\frac{dT}{dz} = N(B - T) \quad (1)$$

Where: (x0, y0, and z0) is the position of a magnetic source whose total field T is detected at (x,y,z). The total field has a regional value of B. The degree of homogeneity N may be interpreted as a structural index. The value of the structural element varies from 0 to 3. The appropriate form of the Euler's equation can be written as follows:

$$(X - X_0)\frac{dT}{dX} + (y - y_0)\frac{dT}{dy} + (z - z_0)\frac{dT}{dz} = A \quad (2)$$

Where: A incorporates amplitude, strike, and dip factors.

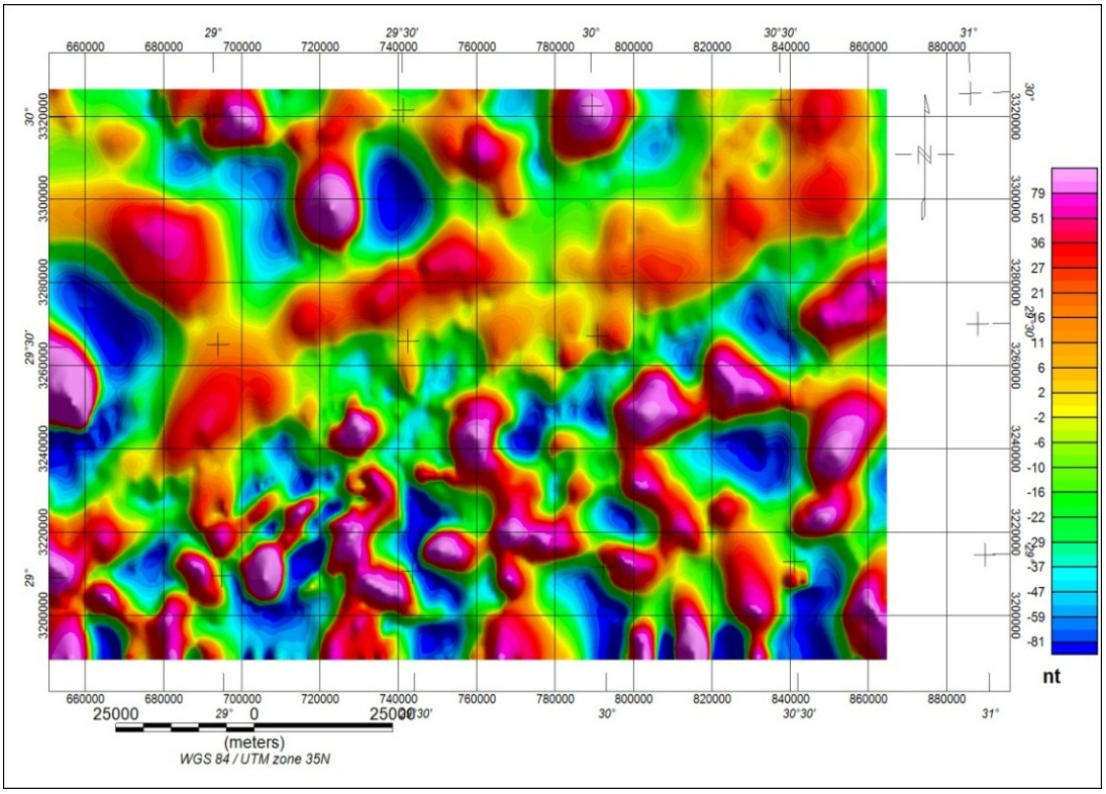

Figure (8): The residual RTP magnetic map after applying the Butterworth filter.

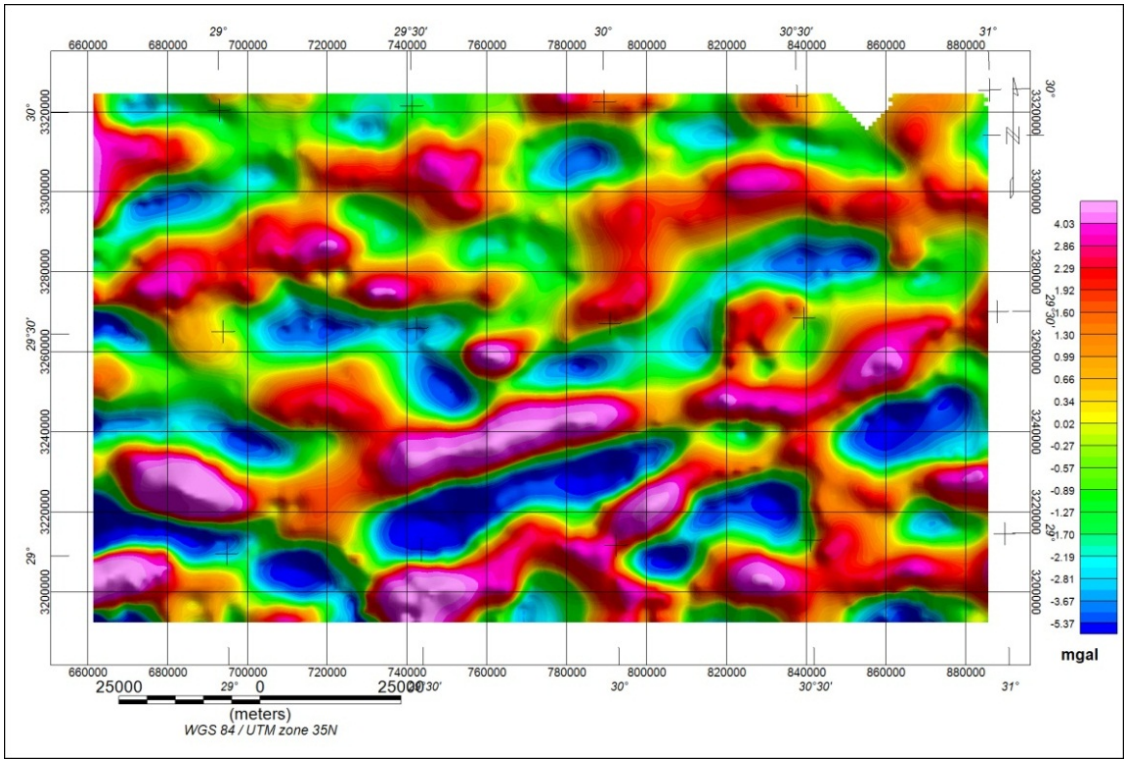

Figure (9): The residual gravity map after applying the Butterworth filter.

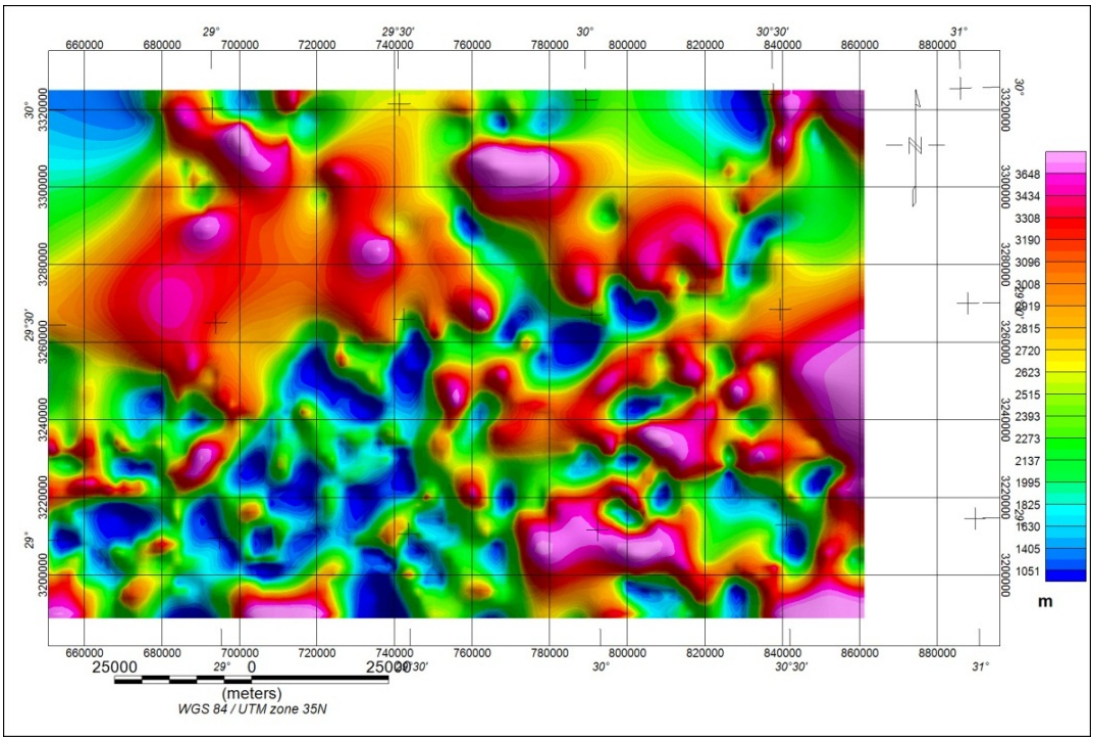

Figure (10): Euler basement depth color shaded map.

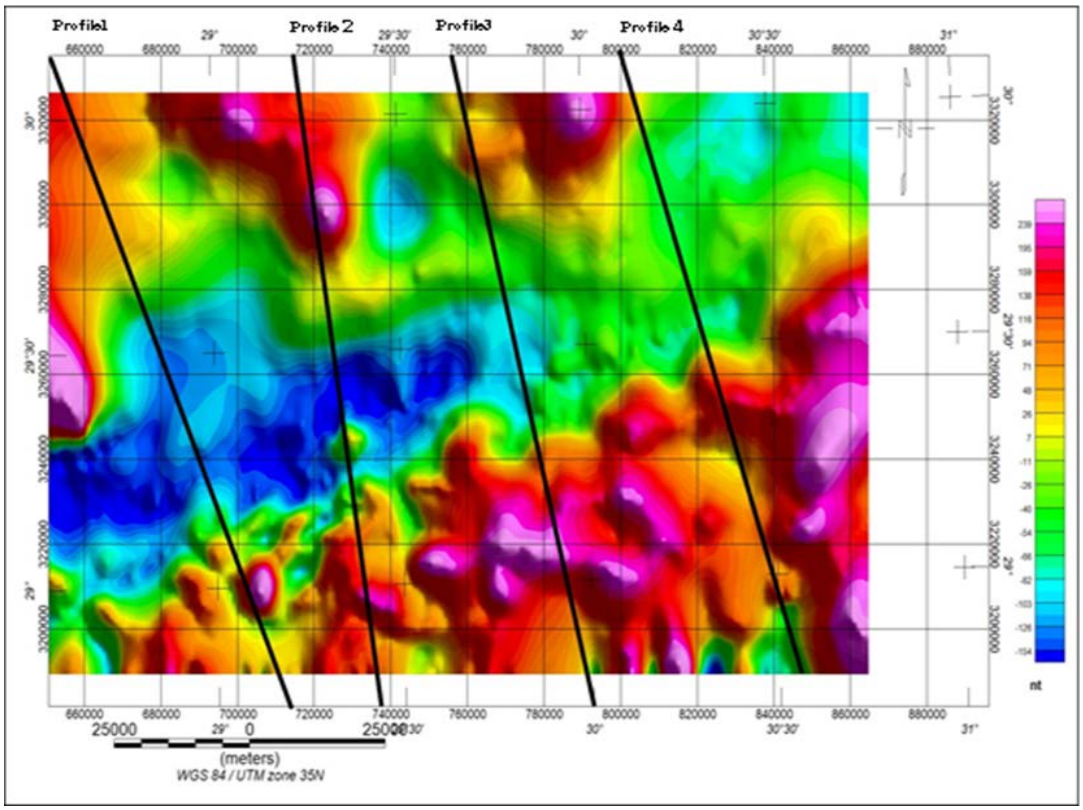

Figure (11): RTP map showing four profiles.

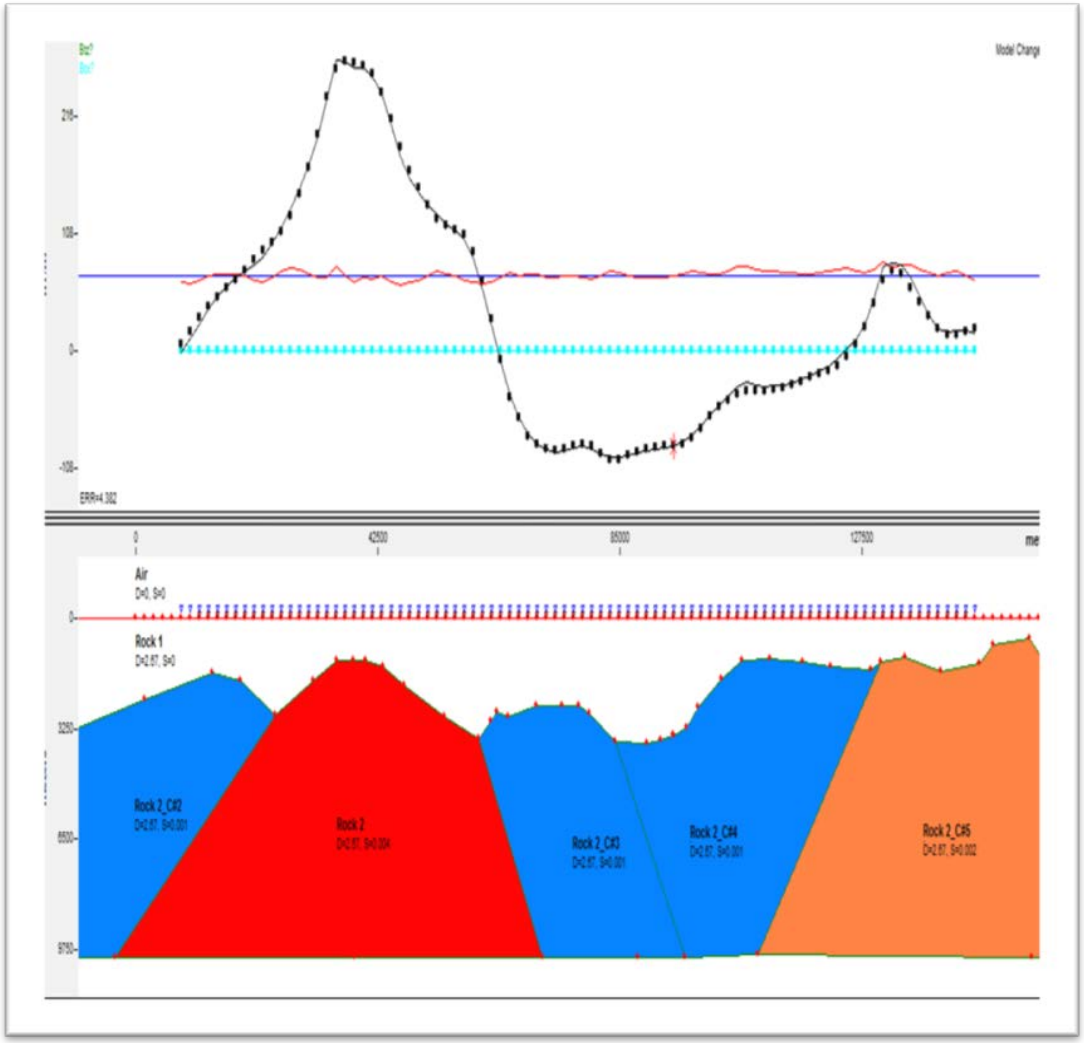

Figure (12): Profile (3) and the constructed 2D model.

Specification of the structural index permits the equation to be solved for source position within a given data window. This window is progressively "moved" across the magnetic data grid, and solutions are generated within each. The process is repeated for various window sizes and structural indices, and the optimum parameters for the data set are determined by clustering of output depth solutions and the comparison with other available information. Structural index values of 0 and 1 were used for various window size tests. An index of 0 solves for source position attributed to geological contacts of significant depth extent (with respect to depth), whereas an index of 1 will identify contacts of limited depth extent (with respect to depth) and dykes or sills (Reid et al., 1990).The basement depth map calculated using the above mentioned technique is shown in figure (10).

Modeled profiles:

Magnetic modeling was carried out along selected profiles oriented NW-SE. The location of The modeled profiles are shown in figures (11) one of the modeled profiles is shown in figure (12). The upper half of the modeled profile represents the observed and calculated RTP anomalies, and the lower part represents the basement blocks that caused the magnetic anomalies. The profile shows an excellent fit between the observed and the calculated magnetic fields and the susceptibilities of basement blocks range between (0.001-0.004 c.g.s). The average magnetic susceptibility of basement blocks is about 0.001-0.002 c.g.s units, which represents granitic composition which is assigned a blue color. An intrabasement blocks with higher susceptibility ranges between 0.004-0.005 c.g.s units, associated with high magnetic anomalies represent granite intruded by basic dykes and are assigned a red color. The basement blocks are extended down to a depth of 10 km to compensate the regional effect and to reach the approximate depth of Curie temperature. The modeled profiles show a good agreement between the depth calculated from 3-D Euler deconvolution techniques and that resulted from modeling. Also the locations of the basin boundaries were confirmed from the modeled profiles.

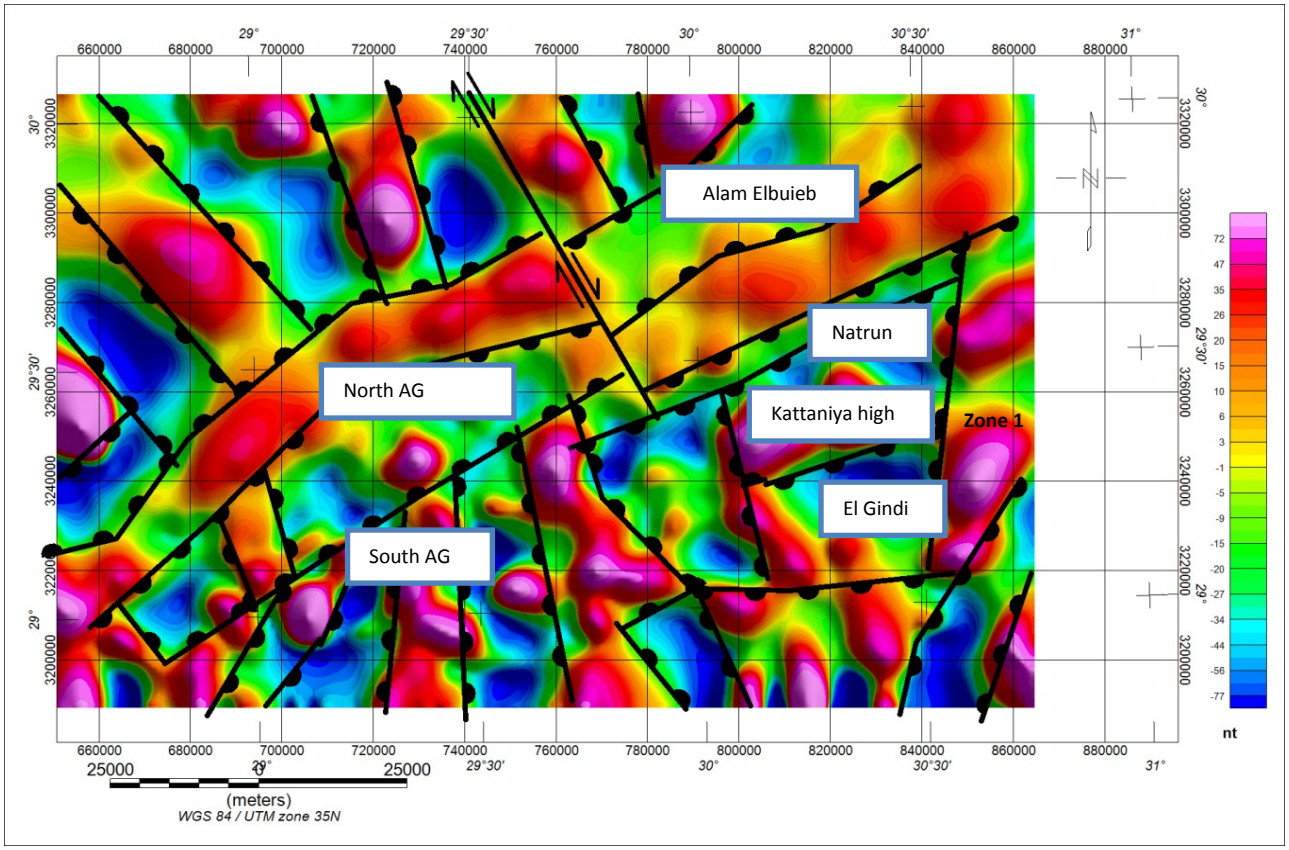

Figure (13): Structural map showing depocenters in the study area.

Interpretation of gravity and magnetic maps:

Detailed mapping and analysis of the structures affecting the Mesozoic and Cenozoic rocks of the North Western Desert indicate three main tectonic deformations affected the northern Western Desert during the Mesozoic and Cenozoic (Moustafa, 2008). These are:

1. Jurassic and Early Cretaceous rifting by NNE-SSW, NE-SW and ENE- WSW oriented faults.
2. Late Cretaceous-early Tertiary positive structural inversion(NNW-SSE and NW-SE).
3. Miocene and post-Miocene extension in the NE-SW direction.

Regional potential field data were interpreted to delineate the main structures in the studied area (Figure 6 and 8). Faults were traced to follow the high gradient on the maps. Folds are qualitatively interpreted as elongated gravity anomalies. High gravity anomalies are associated with uplifted anticlinal structures. On the other hand, low gravity anomalies are associated with synclinal structures, A set of faults having different trends were delineated in the area. The major structural trends are revealed in the studied area .

The structural interpreted basin distribution map Figure (13) was checked against the depth to magnetic basement map (Figure 10) that was constructed from gridded RTP magnetic file applying Euler deconvolution technique and checked by 2-D modeling. Excellent correlation between both maps is evident which gives more confidence in both of them. The following are the major depocenters:

There are two main dominant trends which are NW-SE and NE-SW. The structure interpretation map(figure 13) shows a series of uplifted and down faulted blocks in the form of horst and graben the uplifted blocks associated with the Kattaniya high trending in the NE-SW . This zoneis affected by a strike slip (right lateral) fault trending NW-SE. This zone attains a depth to basement of 1000m. South of Kattaniya high, there is a depocenter associated with El- Gindi basin trending NE-SW. The basement depth attains a maximum of more than 3000-4000 m. Another basinal area is associated with Abu Gharadig basin. The residual gravity anomaly maps shows that the AG basin is separated into two anomalies one to the south and the other one to the north . The two basins are separated by high structure . Natrun basin is located to the north of El Gindi basin and both are separated by the Kattaniya high. The Natrun Basin is trending NE-SW and attains a depth to basement of 3000 m or more.

In the northern part of the area ,there is a part of Alam el Bueib basin trending ENE-WSW

and attains a depth more than 3000 m. It is separated from Natrun basin by an uplifted block trending NE-SW . (kattaniya high) which ispropably affected by a

strike slip (right lateral) fault trending NW-SE. It attains a depth to basement of 1000 to 2000 m.

CONCLUSION

Depth to basement using Euler deconvolution automatic techniques were calculated. Qualitative interpretation was done to relate the different anomalies to their possible geologic causes. 2-D modeling along four selected profiles were designed to evaluate the possible locations of the faults and basement surface. Finally a depth map for the basement was contoured from these models .Gravity and Magnetic maps digitized and gridded for data processing . Different filters (regional-residual , band-pass and derivative) applied to enhance the data and making features easier to recognize. Depth to basement using different automatic techniques (Euler deconvolution and Source Parameter Imaging (SPI)) were calculated and adjusted by 2-D modeling along selected profiles. Interpretation of the potential field data to delineate the major structures and define the expected sedimentary basins.

Basement tectonic map shows alternating uplifted and down-faulted blocks trending ENE-WSW. The two uplifted zones are denoted by zone I and zone II from the north to the south respectively. Zone I and zone II are separated by a normal fault trending ENE-WSW with the downthrow in the direction of zone II. The ENE-WSW structures are intersected by a series of NW-SE trending faults.

There are two main dominant trends, these are NW-SE and NE-SW. They comprise a series of uplifted and down-faulted blocks in the form of horsts and grabens. One of The uplifted blocks is associated with the Kattaniya high trending NE-SW . This zone is probably dissected by a strike- slip (right- lateral) fault trending NW-SE. This zone attains a depth to basement of 1000 m. South of Kattaniya high there is a depocentar associated with El-Gindi basin trending NE-SW with basement depth attains a maximum of 4000 m. Another basinal area is associated with Abu-Gharadig (AG) basin and attains a depth of (3000-6000) m. The residual gravity anomaly map shows that the AG basin is separated into two anomalies one to the south and the other one to the north .The two anomalies are separated by high structure . Natrun basin is located to the north of Gindi basin and both are separated by Kattaniya high. Natrun basin is trending NE-SW and attains a depth to basement more than 3000 m. In the northern part of the area ,there is a part of Alam el Bueib basin trending in ENE-WSW and attains a depth more than 3000 m. It is separated from Natrun basin by an uplifted block trending NE-SW. This zone was probably affected by a strike- slip (right- lateral) fault trending NW-SE.

REFERENCES

Blakly, R.J., 1995, Potential theory in gravity and magnetic applications: Cambridge Univ. Press.

Meshref, W., 1990, Tectonic framework of Egypt: in Said, R., The geology of Egypt, Balkima, the Netherlands.

Milligan, P.R., Gunn, P.J., 1997, Enhancement and presentation of airborne geophysical data. AGSO Journal of Australian Geology & Geophysics, 17(2), 63-75.

Moustafa, A.R., 2008, Mesozoic-Cenozoic Basin Evolution in the Northern Western Desert of Egypt in : Geology of East Libya, vol. 3, pp. 29-46 .

Nettleton, L. L., 1976, Gravity and magnetics in oil prospecting: McGraw-Hill, New York.

Reid, A.B., Allsop, J.M., Granser, H., Millett, A.J. and Somerton, I.W., 1990, Magnetic interpretation in three dimensions using Euler deconvolution: Geophysics, 55, 80-91.

Said, R., 1962, The Geology of Egypt. Elsevier, Amsterdam, 377 p.

Thompson, D.T., 1982, EULDPH: A new technique for making computer-assisted depth estimates from magnetic data: Geophysics, 47, 31-37.